MINERALOGICAL MAGAZINE, JUNE 1969, VOL. 37, NO. 286

Physical properties of synthetic and natural pyroxenes in the system diopside–hedenbergite–acmite

J. NOLAN

Department of Geology, The Johns Hopkins University, Baltimore, Maryland, U.S.A.[1]

SUMMARY. Unit cell dimensions and refractive indices have been determined for synthetic pyroxenes in the system $CaMgSi_2O_6$–$CaFeSi_2O_6$–$NaFeSi_2O_6$, which have been crystallized and annealed on the nickel–bunsenite (Ni–NiO) oxygen buffer curve at 700 °C and a total pressure of 2 kb. The data presented confirms the many postulates that a complete solid solution series does exist in the subsolidus region of the 'ternary' system. The unit cell dimensions show an almost linear change with composition between the end members. The determined cell parameters for a series of analysed natural alkali pyroxenes have been compared with the data for the synthetic pyroxenes and close agreement was found between both sets of data. The variation of the unit cell dimensions and refractive indices has been examined in relation to the possible ionic substitutions taking place in the pyroxenes.

AEGIRINE and aegirine-augite crystallize in a number of distinct and contrasted parageneses. They are found in alkaline igneous complexes and associated pegmatites, regionally metamorphosed assemblages, and acmite has been reported as an authigenic mineral from the Green river formation in Colorado, Wyoming, and Utah (Milton and Eugster, 1959). In general, however, they occur pre-eminently as the products of late crystallization of alkaline magmas.

Vogt (1924) was one of the first investigators to infer that there should be a complete solid-solution series in the system Di(diopside)–Hd(hedenbergite)–Ac(acmite). Yagi (1953) from a study of alkali pyroxenes from the alkalic rocks of the Morotu District, Sakhalin, and later (1966) from experimental work along the join diopside–acmite also suggested that there may be continuous solid solution between the end members of the alkali pyroxenes in question.

Aoki (1964, p. 1214), however, concluded on the basis of plotting several alkali pyroxenes in terms of Na, Fe, Mg, that the fields of Na and Ca pyroxenes are separated by a wide region of immiscibility under igneous conditions.

As far as the author is aware no systematic experimental data are available for the 'ternary' compositions in the system Di–Hd–Ac; experimental data are, however, available for two of the bounding joins, diopside–hedenbergite (Turnock, 1962) and diopside–acmite (Yagi, 1962, 1966; Nolan and Edgar, 1963). Coleman (1962) presents cell-size data for various diopsides in which Na^+ and Mg^{2+} have been substituted for Ca^{2+}; Al^{3+}, Fe^{3+}, and Ti^{4+} for Mg^{2+}; and Al^{3+} and Fe^{3+} for Si^{4+}. Schüller (1958) presents data for a more limited range of ionic substitutions in diopside.

---

[1] Present address: The Department of Geology, Imperial College of Science and Technology, South Kensington, London SW. 7.

Nomenclature. The names acmite and aegirine for the purpose of this investigation are not used in a synonymic sense; acmite refers to the hypothetical or synthetic end-member component $NaFeSi_2O_6$, whilst aegirine is used to denote a compositional variation in the alkali pyroxene series. Although the 'molecules' acmite ($Na_2O.Fe_2O_3.4SiO_2$), diopside ($CaO.MgO.2SiO_2$) and hedenbergite ($CaO.FeO.2SiO_2$) are the end-member pyroxenes under discussion, jadeite ($Na_2O.Al_2O_3.4SiO_2$) and the Ca Tschermaks molecule $CaAl(AlSi)O_6$ do in some cases reach significant proportions in the natural alkali pyroxenes.

There is no general agreement on the nomenclature of the intermediate alkali pyroxenes. The nomenclature of the alkali pyroxenes used in this paper is based on that proposed by Washington and Merwin (1927): for pyroxenes containing more than 80 % of the end members, the pyroxene is called by the name of the end member (apart from the acmite–aegirine modification discussed above); where the pyroxene contains dominantly two of the end members and less than 10 % of the third, such names as diopsidic acmite are used; when all three end members are present in amounts other than those previously ascribed the name aegirine-augite is applied.

Experimental techniques. Starting materials were in the form of co-precipitated gels. The method of making homogeneous iron-bearing gels has been described in a previous publication (Nolan and Edgar, 1963) and is a modification of the method described by Roy (1956). Baker 'reagent' grade chemicals were used as source materials. Compositions containing appreciable amounts of the hedenbergite end member were reduced by passing hydrogen over the gels at about 600 °C for two hours; in this way metallic iron was formed; starting materials reduced in this manner were found to be more reactive than the gels in the oxidized state (see Ernst, 1962). Standard hydrothermal cold-seal pressure vessels were used. Heat was supplied by external electric furnaces, temperature being controlled by both on-off and variable-resistance regulators. Temperatures were measured by chromel-alumel thermocouples on a standard potentiometer. Each furnace, pressure vessel, and thermocouple unit was precalibrated and periodically checked against the melting point of sodium chloride (800·5 C°). A large pressure reservoir ensured relatively constant pressure, which was estimated to have been within 40 bars of the stated value.

To avoid the loss of iron from the charges during the experiments the three-tube technique of Eugster and Wones (1962) was used. The pyroxenes were crystallized and annealed at 700 °C (±5 °C) and 2 kb total pressure for 10–14 days. The nickel–bunsenite (Ni–NiO) oxygen buffer assemblage was used to control the oxygen fugacity (f_{O_2}) during the experiments; the control of f_{O_2} was found to be necessary owing to the formation of andradite+quartz+magnetite and/or hematite from hedenbergite compositions at higher values of f_{O_2}.

Optical determinations. The charges were initially inspected for homogeneity using refractive index liquids and a petrographic microscope. In all cases only a single pyroxene phase was determined.

The refractive index α and in some cases γ were determined using either the single variation method of Emmons (1926) or that of Merwin (1922). A petrographic flat stage heating cell similar to that described by Emmons (1926) was used. Owing to the small size of the synthetic crystals, the high dispersion of pyroxenes with high contents of acmite and hedenbergite, and the flat stage determination of the refractive indices, the errors are probably ±0·003 for the indices quoted.

X-ray methods. X-ray determinations of the pyroxenes were made on a Norelco high-angle diffractometer equipped with a curved crystal focusing monochromator. A high intensity Cu tube was used as the X-ray source. Both silicon and calcium fluoride[1] were used as internal standards; the calcium fluoride was used for the hedenbergitic pyroxenes, when the $53\bar{1}$ reflection of the pyroxene tended to mask the 311 reflection of the silicon. The reflections of the end-member pyroxenes, acmite, diopside, and hedenbergite were indexed (on the basis of a *C2/c* space group) by calculation of all possible 2θ values using approximate cell dimensions.

The cell dimensions were calculated using a least squares refinement programme written by Burnham (1962).

The join diopside–hedenbergite. Turnock (1962) determined the phase relations in the system diopside–hedenbergite and confirmed the existence of a complete series of monoclinic pyroxenes in the subsolidus region. The Mg-rich pyroxenes melt through a temperature interval, while compositions richer than about 60 ml. % in the hedenbergite molecule do not melt but invert to a series of wollastonite solid solutions.

From a knowledge of the diopside structure and the crystal chemistry of the pyroxene group in general, predictions can be made as to the particular cell dimensions effected by certain ionic substitutions. A substitution of Mg^{2+} (r^{vi} 0·70 Å) by Fe^{2+} (r^{vi} 0·74 Å) should lead to an increase in the *b* dimension of the pyroxene.

Kuno and Hess (1953) found that for natural pyroxenes Fe^{2+} enrichment results in an increase of *a*, *b*, and the angle β, but has little effect on *c*. Brown (1960) found a linear increase in the *b* dimension as Fe^{2+} substitutes for Mg^{2+} in the clinopyroxene structure for a series of natural pyroxenes along the Ca_{44} compositional line in the system diopside–hedenbergite–enstatite–ferrosilite.

The cell dimensions and optical data for this present investigation are given in table I and are plotted in figs. 1 and 2 respectively. The cell dimensions vary almost linearly with composition; the change in the *a* dimension shows the greatest departure. It can be seen that the variation of the *b* parameter with composition is in general accord with the previous studies, the increase is linear and can be expressed by the equation: $b = 8{\cdot}924+0{\cdot}00103\,(100-di)$, where *di* is the mol % diopside.

The data for the three natural pyroxenes E, F, and G, determined by Kuno and Hess (1953) and later discussed by Brown (1960) have been included in fig. 1 together with specimen H (Kuno, 1955).

Specimens E and F fit the determined curves for the synthetic pyroxenes reasonably well, H however, lies well below both the *a* and *b* curves; this is almost certainly due to a high value of Al^{3+} present in six-fold co-ordination (0·065 Al^{3+} atoms to six oxygens). Specimen G is the hedenbergite from Herault, California (Kuno and Hess,

---

[1] The calcium fluoride (Baker 'Analysed' grade, Lot No. 91548) was annealed for one hour at 800 °C, then calibrated against diamond by D. R. Wones of the United States Geological Survey (*a* 5·4620±0·0005 Å).

TABLE I. *Unit cell parameters and refractive indices α and γ for synthetic pyroxenes on the join diopside–hedenbergite*

Composition mol. %	*a*	*b*	*c*	*β*	*V*	α	γ
Di_{100}	9·748 Å	8·924 Å	5·251 Å	105·79°	439·48 Å³	1·664	1·694
$Di_{91·16}Hd_{8·84}$	9·759	8·934	5·254	105·77	440·86	1·671	1·701
$Di_{82·09}Hd_{17·91}$	9·765	8·941	5·250	105·68	441·32	1·679	1·706
$Di_{72·78}Hd_{27·22}$	9·780	8·954	5·253	105·59	443·08	1·688	1·713
$Di_{63·21}Hd_{36·79}$	9·793	8·962	5·254	105·50	444·28	1·692	1·719
$Di_{53·39}Hd_{46·61}$	9·804	8·971	5·253	105·46	445·30	1·699	1·726
$Di_{43·30}Hd_{56·70}$	9·809	8·985	5·249	105·28	446·33	1·707	1·732
$Di_{32·93}Hd_{67·07}$	9·821	8·994	5·247	105·13	447·39	1·715	1·738
$Di_{22·26}Hd_{77·74}$	9·826	9·012	5·251	105·01	449·20	n.d.	n.d.
$Di_{11·29}Hd_{88·71}$	9·832	9·018	5·247	104·88	449·61	1·727	1·749
Hd_{100}	9·841	9·027	5·247	104·80	450·69	1·732	1·757

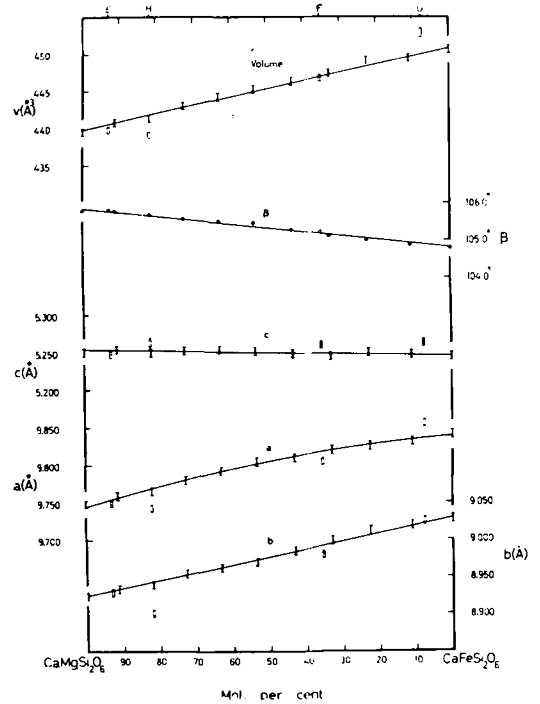

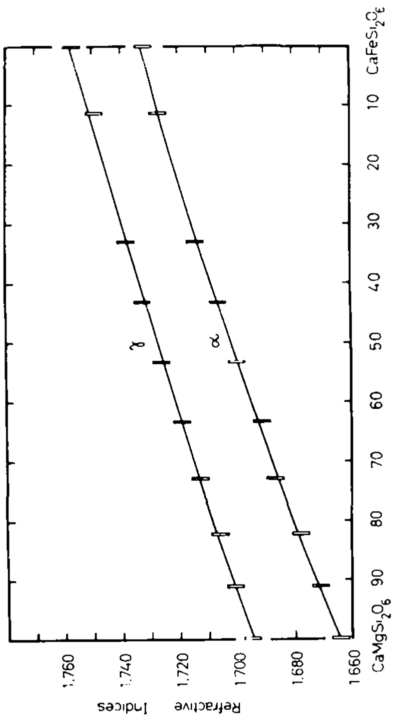

FIGS. 1 and 2: Fig. 1 (left). Unit cell parameters for synthetic and natural pyroxenes on the join diopside–hedenbergite. I denotes synthetic compositions; the length of the symbols indicates the errors of the determination. Open rectangles denote natural specimens (see text). Fig. 2 (right). Variation of refractive indices α and γ for synthetic pyroxenes on the join diopside–hedenbergite.

TABLE II. *Unit cell parameters and refractive index α for synthetic pyroxenes on the join acmite–hedenbergite*

Composition mol. %	*a*	*b*	*c*	*β*	V	α
Ac_{100}	9·658 Å	8·795 Å	5·294 Å	107·42°	429·1 Å^3	1·776
$Ac_{90\cdot63}Hd_{9\cdot37}$	9·671	8·820	5·293	107·21	431·22	1·768
$Ac_{81\cdot12}Hd_{18\cdot88}$	9·691	8·837	5·292	106·95	433·54	1·765
$Ac_{71\cdot48}Hd_{28\cdot52}$	9·707	8·858	5·290	106·78	435·51	n.d.
$Ac_{61\cdot70}Hd_{38\cdot30}$	9·721	8·876	5·282	106·49	437·04	1·757
$Ac_{51\cdot78}Hd_{48\cdot22}$	9·737	8·904	5·278	106·21	439·41	1·749
$Ac_{41\cdot72}Hd_{58\cdot28}$	9·757	8·927	5·272	105·96	441·49	1·746
$Ac_{31\cdot52}Hd_{68\cdot48}$	9·784	8·953	5·268	105·60	444·45	1·742
$Ac_{21\cdot17}Hd_{78\cdot83}$	9·804	8·972	5·263	105·40	446·36	1·738
$Ac_{10\cdot66}Hd_{89\cdot34}$	9·828	8·997	5·258	105·07	448·96	1·736
Hd_{100}	9·841	9·027	5·247	104·80	450·69	1·732

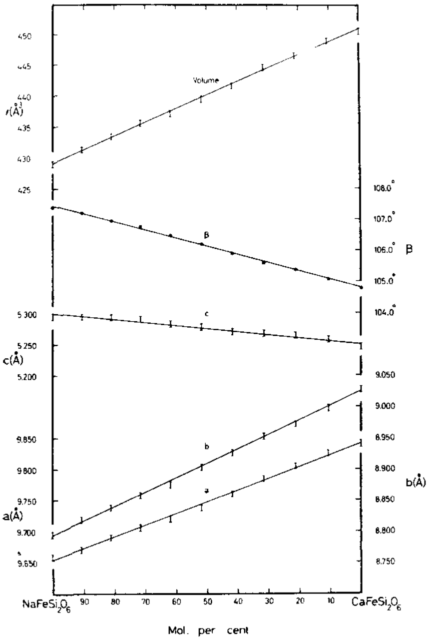

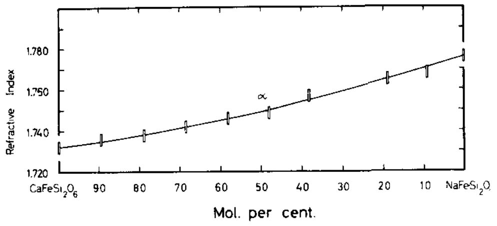

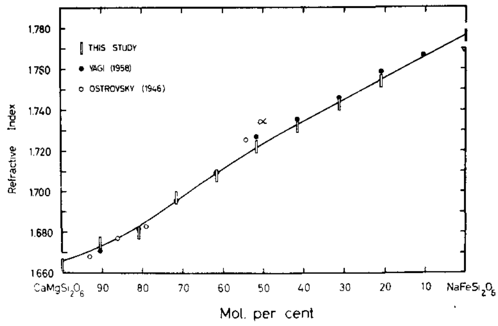

FIGS. 3–5: Fig. 3 (left). Unit cell parameters for synthetic pyroxenes on the join acmite–hedenbergite. Fig. 4 (top right). Variation of refractive index α for synthetic pyroxenes on the join acmite–hedenbergite. Fig. 5 (bottom right). Variation of refractive index α for synthetic pyroxenes on the join acmite–diopside.

1953), which contains 3·70 wt % MnO; a substitution of Fe^{2+} (0·74 Å) by Mn^{2+} (0·80 Å) could account for the departure of the cell dimensions from the determined curves for the synthetic system.

Sakata (1957) and Clark *et al.* (1962) investigated the change in the unit cell dimensions of pyroxenes in the solid solution series diopside–Ca-Tschermak's molecule $CaAl(AlSi)O_6$ and have shown that the cell parameters a, b, and β decrease while c increases linearly with increase of Al^{3+} substituting for both Si and Mg. Sakata (1957) gives values of a, $-0·016$ Å, b, $-0·028$ Å, and c, $+0·008$ Å per 0·1 Al ions in each position (on the basis of six oxygens), assuming that the increase of c depends only on the Al^{3+} in the Si position and the decrease of a and b only on the Al^{3+} in the Mg position.

TABLE III. *Values of the refractive index* α *for the synthetic pyroxenes on the join acmite–diopside*

Composition mol. %	α	Composition mol. %	α	Composition mol. %	α
Ac_{100}	1·776	$Ac_{48\cdot39}Di_{51\cdot56}$	1·722	$Ac_{18\cdot99}Di_{81\cdot01}$	1·680
$Ac_{78\cdot95}Di_{21\cdot05}$	1·754	$Ac_{38\cdot46}Di_{61\cdot54}$	1·708	$Ac_{9\cdot43}Di_{90\cdot57}$	1·675
$Ac_{68\cdot63}Di_{31\cdot37}$	1·743	$Ac_{28\cdot66}Di_{71\cdot34}$	1·697	Di_{100}	1·664
$Ac_{58\cdot44}Di_{41\cdot56}$	1·732				

Brown (1960) discusses the effect of Al^{3+} on the b dimension for a series of augites and pigeonites and concludes that 0·05 Al^{3+} in six-fold co-ordination can be tolerated in the clinopyroxene structure without significantly changing the b dimension; this is, however, in contradiction to data presented by Sakata (1957), who shows a change in the b dimension of the aluminous diopside containing 0·05 Al^{3+} in six-fold co-ordination to be about $-0·014$ Å from that of pure diopside. Brown (1960) was unable to explain the 'anomalous' b dimension for the diopside from St. Lawrence County, but states that the high value of b cannot be attributed to its low aluminium content. This pyroxene labelled E is plotted in fig. 1. The unit cell data for this specimen do agree reasonably well with the determined curves for the synthetic system. The present author believes that the low aluminium content and the fact that its bulk composition lies close to the diopside–hedenbergite join are responsible for this agreement.

The join acmite–hedenbergite. Previous work on this join is rather scant and no investigation has been carried out over the whole compositional range prior to the present study.

Schüller (1958) investigated a portion of the system from pure acmite to 30 wt % hedenbergite and concluded that only limited solid solution is present in the system. Carmichael (1962), from the distribution of pyroxenes in an Na–Fe^{2+}–Mg diagram, suggests that solid solutions do exist in the acmite–hedenbergite series and that they are more common in natural pyroxenes than that between acmite and diopside.

The present investigation confirms the presence of a complete solid-solution series in the subsolidus region of the system. The pyroxenes synthesized along the join are intensely green, with a tendency for the colour intensity to increase towards the hedenbergite end of the series.

The cell parameters and refractive indices for compositions along this join are given in table II and are shown plotted in figs. 3 and 4 respectively. The unit cell dimensions are in complete agreement with the changes predicted for the ionic substitutions taking place; with the replacement of $Ca^{2+}Fe^{2+}$ for $Na^{+}Fe^{3+}$, *a*, *b*, and the volume show a linear decrease whereas both *c* and β increase linearly with composition from hedenbergite to acmite. Due to the coupled nature of the ionic substitutions it is difficult to assign specific effects to the individual ionic substitutions.

TABLE IV. *Unit cell parameters and refractive index* α *for synthetic pyroxenes in the system diopside–hedenbergite–acmite*

Composition mol. %	*a*	*b*		β	V	α
$Di_{10\cdot67}Hd_{9\cdot31}Ac_{80\cdot02}$*	9·679 Å	8·831 Å	5·286 Å	106·96°	432·20 Å³	1·759
$Di_{10\cdot93}Hd_{42\cdot95}Ac_{46\cdot12}$	9·738	8·902	5·277	106·25	439·21	1·742
$Di_{11\cdot05}Hd_{57\cdot87}Ac_{31\cdot08}$	9·764	8·936	5·266	105·80	442·08	1·735
$Di_{11\cdot21}Hd_{78\cdot28}Ac_{10\cdot51}$	9·915	8·990	5·257	105·22	447·61	1·731
$Di_{16\cdot01}Hd_{13\cdot97}Ac_{70\cdot02}$*	9·698	8·848	5·284	106·78	434·07	1·751
$Di_{21\cdot34}Hd_{18\cdot63}Ac_{60\cdot03}$*	9·700	8·859	5·279	106·69	434·52	1·747
$Di_{21\cdot95}Hd_{57\cdot48}Ac_{20\cdot57}$	9·777	8·957	5·265	105·66	443·92	1·728
$Di_{26\cdot77}Hd_{23\cdot26}Ac_{49\cdot97}$*	9·715	8·883	5·278	106·41	436·92	1·737
$Di_{27\cdot24}Hd_{47\cdot34}Ac_{25\cdot42}$	9·764	8·937	5·262	105·81	441·74	1·725
$Di_{32\cdot02}Hd_{27\cdot95}Ac_{40\cdot03}$*	9·733	8·899	5·269	106·19	438·25	1·730
$Di_{32\cdot13}Hd_{32\cdot72}Ac_{35\cdot14}$	9·737	8·909	5·271	106·15	439·16	1·728
$Di_{32\cdot24}Hd_{37\cdot53}Ac_{30\cdot23}$	9·751	8·922	5·262	105·98	440·12	n.d.
$Di_{32\cdot70}Hd_{57\cdot08}Ac_{10\cdot22}$	9·795	8·972	5·258	105·39	445·52	1·718
$Di_{41\cdot84}Hd_{9\cdot13}Ac_{49\cdot03}$	9·710	8·879	5·269	106·39	435·84	1·727
$Di_{42\cdot12}Hd_{18\cdot39}Ac_{39\cdot49}$	9·738	8·904	5·262	106·06	438·52	1·723
$Di_{42\cdot70}Hd_{37\cdot28}Ac_{20\cdot02}$*	9·761	8·937	5·261	105·82	441·53	1·716
$Di_{48\cdot05}Hd_{41\cdot94}Ac_{10\cdot01}$*	9·770	8·949	5·253	105·62	442·35	1·706
$Di_{52\cdot49}Hd_{22\cdot91}Ac_{24\cdot60}$	9·747	8·919	5·264	106·00	439·90	1·711
$Di_{61\cdot95}Hd_{9\cdot01}Ac_{29\cdot04}$	9·728	8·902	5·261	106·15	437·59	1·705
$Di_{62\cdot79}Hd_{27\cdot40}Ac_{9\cdot81}$	9·763	8·941	5·256	105·73	441·55	1·699
$Di_{72\cdot05}Hd_{13\cdot48}Ac_{14\cdot47}$	9·746	8·924	5·263	105·92	440·14	1·694
$Di_{81\cdot55}Hd_{8\cdot89}Ac_{9\cdot56}$	9·744	8·925	5·258	105·88	439·79	1·685

* Denotes synthetic compositions plotted in fig. 9.

The join acmite–diopside. Yagi (1962, 1966) determined the phase relations in the system and found complete solid solution in the subsolidus region of the join. At temperatures near the liquidus, however, the phase relations for acmite rich compositions become complex due to the incongruent melting behaviour of the acmite component. Nolan and Edgar (1963) determined the unit-cell dimensions of pyroxenes synthesized along the join; the data has been recalculated in terms of mol % and used in plotting the variation of the *b* dimension with composition for the ternary system.

TABLE V. *Unit cell parameters and refractive index α for analysed alkali pyroxenes from Uganda and Rockall*

Specimen number	Composition mol. %	$\mathrm{Al}^{\mathrm{iv}}$	$\mathrm{Al}^{\mathrm{vi}}$	*a*	*b*	*c*	β	V	α
N 103 F	$\mathrm{Di}_{5\cdot71}\mathrm{Hd}_{8\cdot17}\mathrm{Ac}_{86\cdot12}$†	0·056	0·052	9·672 Å	8·810 Å	5·292 Å	107·21°	430·79 Å³	1·768
N 103 C	$\mathrm{Di}_{8\cdot50}\mathrm{Hd}_{2\cdot02}\mathrm{Ac}_{89\cdot48}$†	0·069	0·000	9·669	8·816	5·299	107·19	431·53	1·765
To 17	$\mathrm{Di}_{14\cdot67}\mathrm{Hd}_{12\cdot19}\mathrm{Ac}_{73\cdot14}$†	0·035	0·000	9·675	8·837	5·287	106·89	432·58	1·758
To 21	$\mathrm{Di}_{17\cdot33}\mathrm{Hd}_{23\cdot26}\mathrm{Ac}_{59\cdot41}$†	0·000	0·000	9·704	8·863	5·282	106·65	435·32	1·743
To 585	$\mathrm{Di}_{19\cdot32}\mathrm{Hd}_{35\cdot26}\mathrm{Ac}_{45\cdot42}$	0·057	0·060	9·733	8·899	5·280	106·18	439·25	1·720
To 1	$\mathrm{Di}_{21\cdot97}\mathrm{Hd}_{24\cdot20}\mathrm{Ac}_{53\cdot83}$†	0·056	0·000	9·718	8·885	5·277	106·41	437·11	1·740
B 101	$\mathrm{Di}_{32\cdot00}\mathrm{Hd}_{37\cdot15}\mathrm{Ac}_{30\cdot85}$	0·000	0·000	9·761	8·925	5·271	105·95	441·60	1·720
B 68	$\mathrm{Di}_{34\cdot51}\mathrm{Hd}_{31\cdot46}\mathrm{Ac}_{34\cdot03}$†	0·043	0·017	9·748	8·919	5·269	106·03	440·28	1·717
B 33	$\mathrm{Di}_{42\cdot29}\mathrm{Hd}_{36\cdot09}\mathrm{Ac}_{21\cdot62}$†	0·009	0·000	9·766	8·928	5·279	105·70	443·19	1·705
N 62	$\mathrm{Di}_{58\cdot77}\mathrm{Hd}_{20\cdot38}\mathrm{Ac}_{20\cdot85}$	0·120	0·059	9·762	8·926	5·269	105·78	441·80	1·696
N 163	$\mathrm{Di}_{69\cdot91}\mathrm{Hd}_{16\cdot67}\mathrm{Ac}_{13\cdot42}$	0·095	0·000	9·768	8·932	5·267	105·73	442·39	1·681
N 520	$\mathrm{Di}_{70\cdot04}\mathrm{Hd}_{16\cdot60}\mathrm{Ac}_{13\cdot36}$	0·000	0·000	9·763	8·930	5·263	105·77	441·59	1·692
N 170	$\mathrm{Di}_{78\cdot27}\mathrm{Hd}_{14\cdot03}\mathrm{Ac}_{7\cdot70}$	0·084	0·000	9·764	8·931	5·259	105·78	441·37	1·660
F 6152	Acmite from aegirine acmite granite, Rockall (Sabine, 1960)	—	—	9·661	8·804	5·297	107·38	429·97	—

Optical data for the pyroxenes from Uganda after Tyler and King, 1967.

† Denotes specimens plotted in fig. 9.

The optical data compiled in table III and plotted in fig. 5 are from the present study; also incorporated in the diagram are data given by Ostrovsky (1946) and Yagi (1958).

The system acmite–hedenbergite–diopside. Twenty-two ternary synthetic compositions in the system were investigated; in all cases only a single phase pyroxene was found to be present. The pyroxenes range in colour from pale green for diopsidic acmites to extremely dark green for hedenbergite-rich compositions, especially those close to the hedenbergite–acmite join.

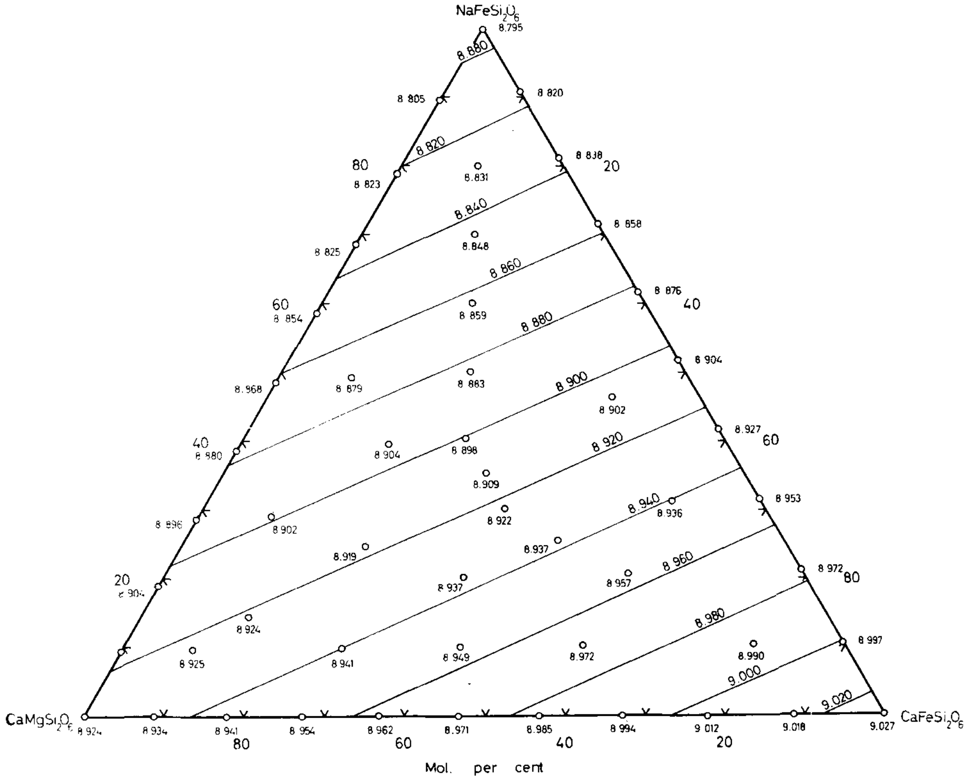

FIG. 6. Variation of the *b* unit cell parameter for synthetic pyroxenes in the system diopside–hedenbergite–acmite.

The unit cell dimensions and optical data are given in table IV. Combining the cell data for the ternary compositions with those determined for the bounding joins, the system was initially contoured for all cell dimensions, but only a plot of the *b* dimension is given contoured at intervals of 0·02 Å (fig. 6). The contoured surface shows an almost linear decrease for the *b* dimension with the substitution of $Ca^{2+}(Mg^{2+},Fe^{2+})$ for $Na^{+}Fe^{3+}$.

Miss R. Tyler kindly supplied the author with thirteen analysed alkali pyroxenes (Tyler and King, 1967), whose compositions when recalculated in terms of the end members acmite, hedenbergite, and diopside sum to 90 % or more of the total pyroxene; these figures were then recast to 100 %. The method for computing their cell parameters was identical with that previously described for the synthetic pyroxenes. The unit cell dimensions are listed in table V, together with a specimen of acmite from the aegirine–acmite granite, Rockall (Spec. No. F 6152), kindly supplied by Dr. P. A. Sabine (Sabine, 1960). The determined *b* dimensions are plotted in fig. 7. Within the limits of experimental error for the determination of the cell parameters ($\pm$0·005 Å) the results for the natural alkali pyroxenes are in good agreement with the determined curves for the synthetic compositions. The *b* dimension of specimen N 103 F would appear to be slightly low; this is probably due to a fairly large amount of Al^{3+} (0·052) present in six-fold co-ordination, which, as discussed previously, results in the decrease of the *b* dimension.

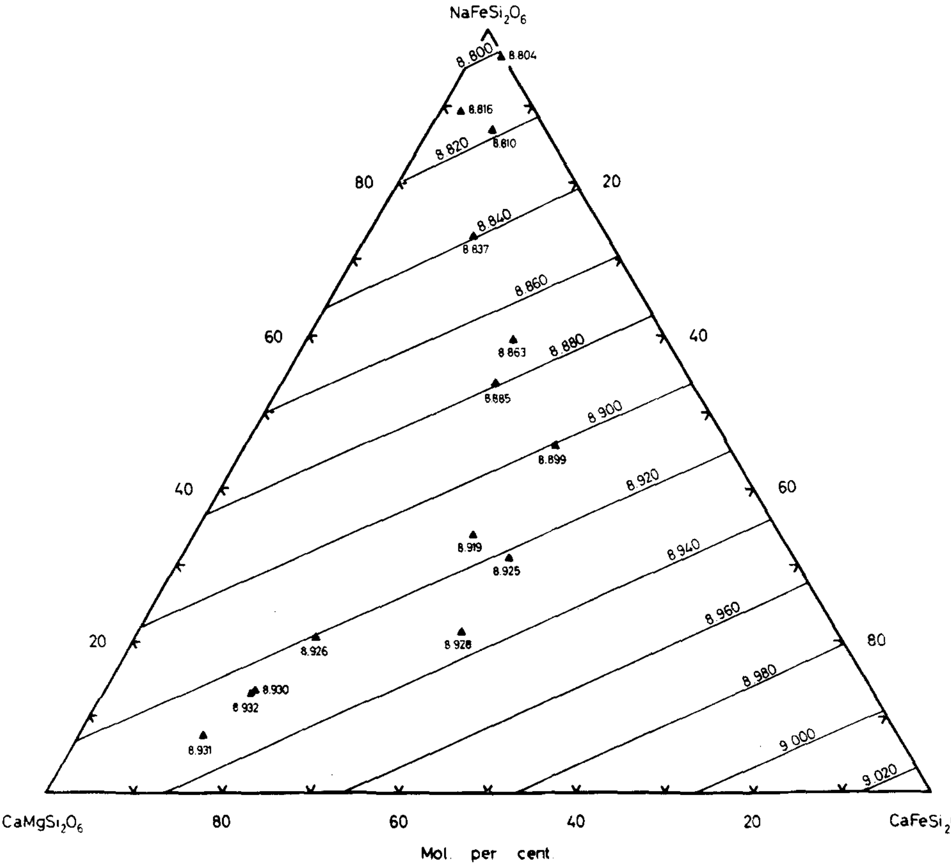

FIG. 7. Plot of the *b* unit cell parameter of natural alkali pyroxenes from Uganda and Rockall (see table V).

The system acmite–hedenbergite–diopside has also been contoured for the refractive index α and is shown in fig. 8. For acmite-rich compositions the values of α show an almost linear increase with increments in that component; there is, however, a marked departure from linearity for compositions close to the diopside apex as was found by Ostrovsky (1946) and Yagi (1958) for pyroxenes along the acmite–diopside join.

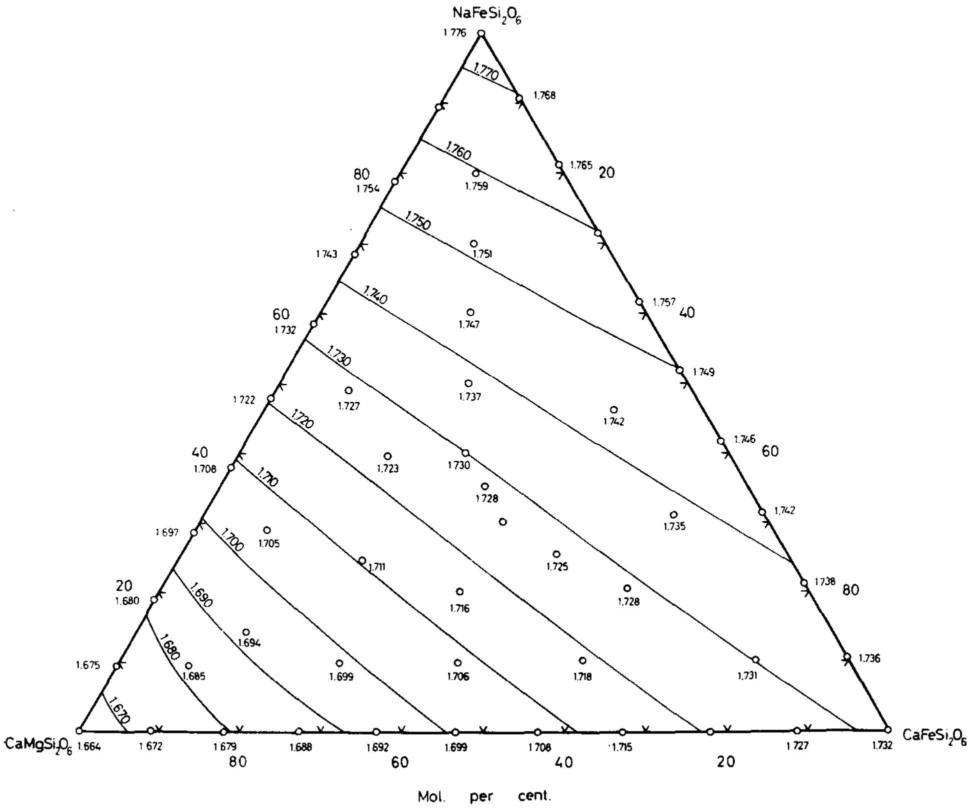

FIG. 8. Variation of the refractive index α for synthetic pyroxenes in the system diopside–hedenbergite–acmite.

Tyler and King (1967) plotted the variation of the refractive index α with composition for a series of alkali pyroxenes from E. Uganda. Their data show a marked lowering of the refractive index, especially for the diopsidic pyroxenes, when compared with the synthetic data. On inspection of the pyroxene analyses it was found that the majority of the diopside-rich pyroxenes have a marked substitution of Si by Al, Ti, and Fe^{3+}, which tends to decrease towards the acmite apex (see also King, 1965). Hori (1954) found that the substitution of such ions in the tetrahedral position significantly lowered the refractive indices of clinopyroxenes, although Al, Ti, and

Fe^{3+} substituting in the octahedral position had the opposite effect (see also Zvetkov, 1945). It was found that many of the diopsidic pyroxenes described by Tyler and King (1967) were so deficient in silicon as to require all the available Al and in addition Ti, and in some cases even Fe^{3+} as well, to satisfy the structural formula. The differences between the optical data for the synthetic and natural pyroxenes discussed above can therefore in most cases be attributed to the substitution by Al, Ti, and Fe^{3+} in the tetrahedral position of the clinopyroxene structure.

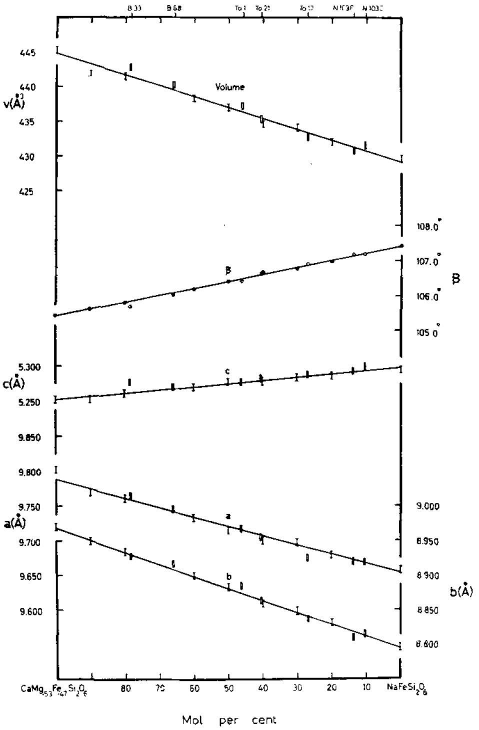

FIG. 9. Variation of the unit cell parameters for synthetic and natural pyroxenes of the 'acmite–aegirine–augite–augite series'. Natural pyroxenes denoted by open rectangles.

In general the course of crystallization of pyroxenes in most alkaline rocks shows some degree of enrichment in the acmite molecule towards the final stages of crystallization, the most extreme case of such a trend so far recorded being that described for the alkalic rocks of the Morotu district, Sakhalin (Yagi, 1953), where the pyroxenes change continuously in composition from diopsidic augite through soda augite and aegirine–augite to aegirine. In view of such pyroxene trends, the unit-cell dimensions of synthetic pyroxenes along the join acmite$_{100}$–diopside$_{50}$ hedenbergite$_{50}$ expressed in wt % (compositions denoted by an asterisk in table IV) and natural pyroxenes with compositions closely approximating to this join (denoted by a dagger in table V) have been plotted in fig. 9, all compositions having been recalculated in terms of mol % of the end members. In the majority of cases the agreement between the synthetic and natural data is within the limits of experimental error for the determination of the cell parameter.

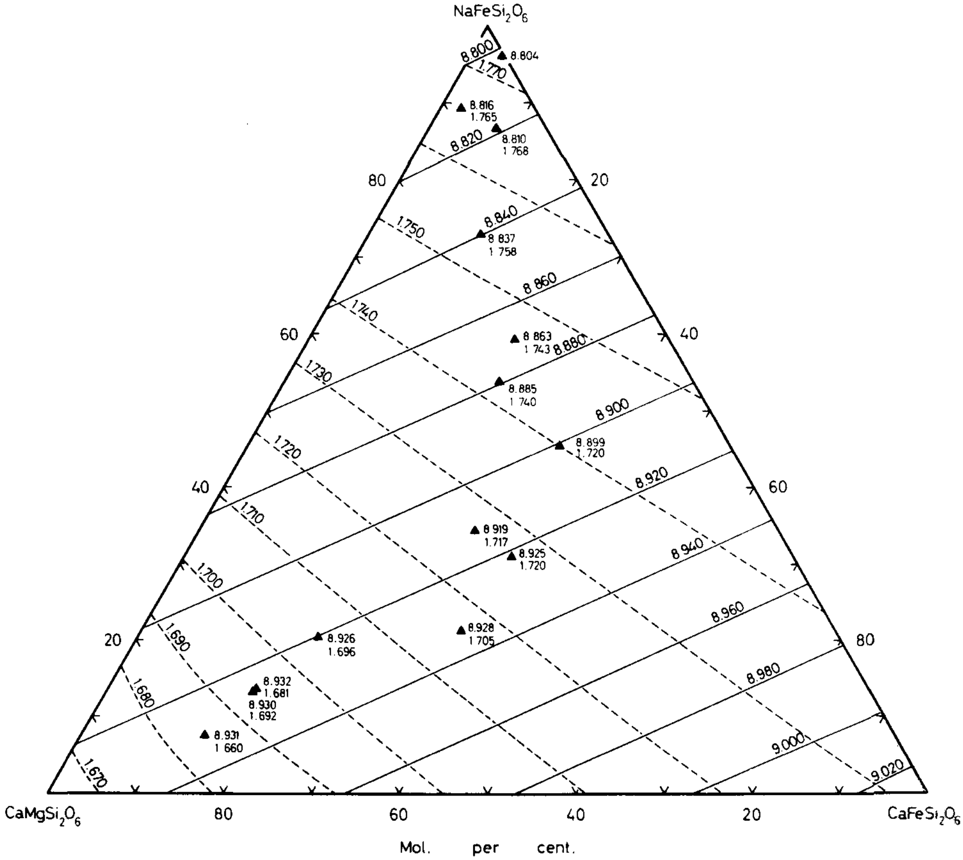

FIG. 10. Relationship between chemical composition and the combined optical and unit cell data for synthetic and natural pyroxenes in the system diopside–hedenbergite–acmite.

Combining the optical and *b* dimension data from figs. 6 and 8, it is possible to determine the composition of synthetic alkali pyroxenes to within about 3 mol % for each of the end members. Because of the necessity of keeping the synthetic system as simple as possible in terms of components, caution must be exercised in directly applying the results of such synthetic studies to the problems of natural mineral assemblages. Both aluminium and titanium, omitted from the synthetic study, have an important influence on the stability of the pyroxenes in question and also on the physical parameters measured in this investigation. Bearing such limitations in mind an attempt was made to redetermine the composition (in terms of the end members Ac–Hd–Di) of a number of analysed natural alkali pyroxenes (see fig. 10).

Providing the aluminium and titanium contents of the pyroxenes are low, reasonable results can be obtained, but with appreciable increase in the substitution of the aluminium and titanium in the pyroxene structure, the errors in determining the composition do become large, the principal error being caused by the acute sensitivity of the refractive indices to the substitution of such cations; this is clearly seen by comparing fig. 7 with the optical data given by Tyler and King (1967, fig. 5).

The experimental evidence shows the presence of a complete solid solution series in the subsolidus region of the system acmite–hedenbergite–diopside, for values of f_{O_2} within the magnetite stability field, specified by the Ni–NiO oxygen buffer at 2 kb total pressure, thereby invalidating the immiscibility gap between Na- and Ca-rich pyroxenes proposed by Aoki (1964).

Acknowledgements. The author expresses his sincere gratitude to Professor Hans P. Eugster for his help and interest during the course of the investigation. Miss R. Tyler and Dr. P. A. Sabine kindly supplied the natural alkali pyroxenes used in this study. The research was supported by two National Science Foundation grants, G.P. 1796 and G.P. 5064. Dr. R. A. Howie very kindly reviewed the manuscript.

REFERENCES

AOKI (A. I.), 1964. *Amer. Min.* **49**, 1199.
BROWN (G. M.), 1960. Ibid. **45**, 15.
BURNHAM (C. W.), 1962. *Carnegie Inst. Wash., Year Book*, **61**, 132.
CARMICHAEL (I. S. E.), 1962. *Min. Mag.* **33**, 86.
CLARK (S. P.), SCHAIRER (J. F.), and NEUFVILLE (J. DE), 1962. *Carnegie Inst. Wash. Year Book*, **61**, 59.
COLEMAN (L. C.), 1962. *Geol. Soc. Amer.*, Buddington volume, 429.
EMMONS (R. C.), 1926. *Amer. Min.* **11**, 115.
ERNST (W. G.), 1962. *Journ. Geol.* **70**, 689.
EUGSTER (H. P.) and WONES (D. R.), 1962. *Journ. Petrology*, **3**, 82.
HORI (F.), 1954. *Sci. Papers College Gen. Education, Univ. Tokyo*, **4**, 71.
KING (B. C.), 1965. *Journ. Petrology*, **6**, 67.
KUNO (H.), 1955. *Amer. Min.* **40**, 70.
—— and HESS (H. H.), 1953. *Amer. Journ. Sci.* **251**, 741.
MERWIN (H. E.), 1922. *Journ. Amer. Chem. Soc.* **44**, 1970.
MILTON (C.) and EUGSTER (H. P.), 1959. *Researches in Geochemistry*. New York (Wiley).
NOLAN (J.) and EDGAR (A. D.), 1963. *Min. Mag.* **33**, 625.
OSTROVSKY (I. A.), 1946. *Acad. Sci. USSR*, D.S. Belyankin Jubilee volume, 505.
ROY (R.), 1956. *Journ. Amer. Ceram. Soc.* **39**, 145.
SABINE (P. A.), 1960. *Bull. Geol. Surv. Gt. Britain*, no. 16, 156.
SAKATA (Y.), 1957. *Jap. Journ. Geol. Geogr.* **28**, 161.
SCHÜLLER (K. H.), 1958. *Beitr. Min. Petr.* **6**, 112.
TURNOCK (A. C.), 1962. *Carnegie Inst. Wash. Year Book*, **61**, 82.
TYLER (R. C.) and KING (B. C.), 1967. *Min. Mag.* **36**, 5.
VOGT (J. H. L.), 1924. *Norsk. Vid. Akad. Oslo, Math. Nat. Kl. Skv.* 15.
WASHINGTON (H. S.) and MERWIN (H. E.), 1927. *Amer. Min.* **12**, 233.
YAGI (K.), 1953. *Bull. Geol. Soc. Amer.* **64**, 769.
—— 1958. *Journ. Min. Soc. Japan*, **3**, 763.
—— 1962. *Carnegie Inst. Wash. Year Book*, **61**, 98.
—— 1966. *Amer. Min.* **51**, 976.
[ZVETKOV (A. I.)] ЗВЕТКОВ (А. И.), 1945. Зап. всесоюз. мин. общ. (*Mém. Soc. Russe Min.*), ser. 2, **74**, 215.

[*Manuscript received 26 July 1968*]